JACS
JOURNAL OF THE AMERICAN CHEMICAL SOCIETY

Article

pubs.acs.org/JACS

Rational Design of Highly Sensitive Fluorescence Probes for Protease and Glycosidase Based on Precisely Controlled Spirocyclization

Masayo Sakabe,[†] Daisuke Asanuma,[‡] Mako Kamiya,[‡] Ryu J. Iwatate,[‡] Kenjiro Hanaoka,[†] Takuya Terai,[†] Tetsuo Nagano,*[,†] and Yasuteru Urano*[,‡,§]

[†]Graduate School of Pharmaceutical Sciences, and [‡]Graduate School of Medicine, The University of Tokyo, 7-3-1 Hongo, Bunkyo-ku, Tokyo 113-0033, Japan

[§]Basic Research Program, Japan Science and Technology Agency, 3-5 Sanbancho, Chiyoda-ku, Tokyo 102-0075, Japan

Supporting Information

ABSTRACT: We have synthesized and evaluated a series of hydroxymethyl rhodamine derivatives and found an intriguing difference of intramolecular spirocyclization behavior: the acetylated derivative of hydroxymethyl rhodamine green (Ac-HMRG) exists as a closed spirocyclic structure in aqueous solution at physiological pH, whereas HMRG itself takes an open nonspirocyclic structure. Ac-HMRG is colorless and nonfluorescent, whereas HMRG is strongly fluorescent. On the basis of these findings, we have developed a general design strategy to obtain highly sensitive fluorescence probes for proteases and glycosidases, by replacing the acetyl group of Ac-HMRG with a substrate moiety of the target enzyme. Specific cleavage of the substrate moiety in the nonfluorescent probe by the target enzyme generates a strong fluorescence signal. To confirm the validity and flexibility of our strategy, we designed and synthesized fluorescence probes for leucine aminopeptidase (Leu-HMRG), fibroblast activation protein (Ac-GlyPro-HMRG), and β-galactosidase (βGal-HMRG). All of these probes were almost nonfluorescent due to the formation of spirocyclic structure, but were converted efficiently to highly fluorescent HMRG by the target enzymes. We confirmed that the probes can be used in living cells. These probes offer great practical advantages, including high sensitivity and rapid response (due to regulation of fluorescence at a single reactive site), as well as resistance to photobleaching, and are expected to be useful for a range of biological and pathological investigations.

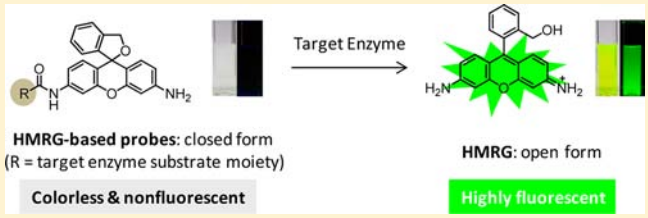

INTRODUCTION

Proteases catalyze the cleavage of specific peptide bonds of their substrates at the cell surface, in cytoplasm, or within various cellular compartments, and many of them play essential roles in physiological functions and also in disease.[1,2] For example, alterations in protease activities or secretion of proteases into extracellular space are thought to be involved in tumor metastasis and inflammation.[3] Sensitive and accurate detection of protease activities in living samples is therefore essential for research in biology and medicine. Fluorescence probes for various protease (aminopeptidase) activities have been developed based on 7-amino-4-methylcoumarin (AMC)[4,5] or Rhodamine Green (RG)[6] and used mainly for *in vitro* experiments, such as biochemical assays. However, these probes are generally unsuitable for application in living cells or *in vivo*. AMC derivatives require ultraviolet (UV) light excitation, which is cytotoxic and induces high background autofluorescence. In contrast, RG-based probes possess favorable characteristics for biological applications, such as longer excitation/emission wavelengths and high fluorescence quantum yield, but these probes normally have two reactive sites, so that two steps of enzymatic reaction are necessary to obtain strongly fluorescent products, and this results in a reduction in the speed and efficiency of fluorescence activation. We recently showed that a spirocyclization design strategy can be utilized to provide fluorescence OFF/ON switches for tetramethylrhodamine and diethylrhodol, leading to probes for hypochlorite[7] and β-galactosidase.[8] However, the potential molecular targets of these probe designs are strictly limited in principle to reactive oxygen species and *O*-directed glycosidases, respectively. Here, we describe a more general spirocyclization design strategy, which overcomes the limitations of the AMC- and RG-based probes, by utilizing the hydroxymethyl rhodamine green (HMRG) scaffold. This is based on our finding that, whereas HMRG itself has an open structure that is highly fluorescent, it predominantly forms a closed spirocyclic structure that is nonfluorescent when one of its amino groups is acetylated (Ac-HMRG). Therefore, by replacing the acetyl group of Ac-HMRG with a suitable substrate moiety, we can obtain novel probes that show strong fluorescence activation upon single-step cleavage of the substrate moiety by the target enzyme. We validated this strategy by developing fluorescence probes for two *N*-directed peptidases, leucine aminopeptidase (LAP) and fibroblast activation protein (FAP). To further show the flexibility of the strategy, we also developed a highly sensitive fluorescence probe for *O*-directed β-galactosidase by using a carbamate functional unit as the substrate moiety. Our findings indicate that the present spirocyclization design strategy has a high degree of generality

Received: October 1, 2012
Published: December 3, 2012

dx.doi.org/10.1021/ja309688m | J. Am. Chem. Soc. 2013, 135, 409−414

and should be suitable to develop probes for imaging a wide range of target molecules in live cells.

RESULTS AND DISCUSSION

Spirocyclization of rhodamine derivatives is a powerful technique for designing fluorescence probes, as the spirocyclized derivative is colorless and nonfluorescent due to separation of the π-conjugation system of the original fluorophore. Fluorescence probes for metal ions, reactive oxygen species, pH, and so on have been developed by utilizing the ring-opening reaction of spirocylized rhodamine upon reaction with the analyte, as this regenerates the original fluorophore, which exhibits strong fluorescence emission.[9−12] Therefore, precise regulation of the equilibrium between the spirocyclic closed form (colorless and nonfluorescent) and the open form (strongly fluorescent) might provide a broadly applicable strategy for controlling the fluorescence. We previously reported that a series of tetramethylrhodamine (TMR) derivatives bearing a hydroxymethyl group instead of the original carboxy group showed unique intramolecular spirocyclization behavior.[7] On the basis of these findings, we aimed to establish a strategy to design fluorescence probes for a wide range of proteases, as well as other enzymes. For this purpose, we required a hydroxymethyl rhodamine derivative that would be predominantly present in the spirocyclic form at physiological pH, thus showing no background fluorescence. We considered that it might be possible to replace the substituent on such a derivative with a substrate moiety for a target enzyme while retaining the closed spirocyclic structure. Next, specific hydrolysis by the target enzyme might release the substrate moiety and convert the spirocyclic structure to the strongly fluorescent open form.

To find a suitable rhodamine derivative, we first prepared a series of hydroxymethyl rhodamines (HMRs) bearing a primary aromatic amine on one side of the xanthene moiety, into which a substrate peptide could be incorporated via an amide bond. The other side of the xanthene moiety was designed to have a primary amine (hydroxymethyl rhodamine green: HMRG), *N*,*N*-dimethylamine (hydroxymethyl dimethylrhodamine: HMDiMeR), or *N*,*N*-diethylamine (hydroxymethyl diethylrhodamine: HMDiEtR) structure, to examine the effect of *N*-alkyl substitution on the optical properties (Figure 1a, Scheme S1). We also prepared the corresponding acetylated derivatives of these three HMRs (Ac-HMRG, Ac-HMDiMeR, Ac-HMDiEtR), which we considered to be models of aminopeptidase substrates (Scheme S2). The optical properties of these HMR derivatives showed strong pH dependency, as in the case of other fluorophores bearing a hydroxymethyl group; the absorption and fluorescence intensity of these HMR derivatives decrease as the pH is increased due to nucleophilic attack of the hydroxymethyl group at the C9 position of the xanthene fluorophore to form the spirocyclic structure (Figures 1b, S1). In other words, HMRs exist in the open form under acidic and neutral conditions, but as the spirocyclic closed form under basic conditions. From pH titration curves, the pK_{cycl} value of HMRs was calculated to be 8.1 for HMRG, 8.9 for HMDiMeR, and 9.3 for HMDiEtR (pK_{cycl} is the pH at which the extent of spirocyclization is sufficient to reduce the absorbance of the compound to one-half of the maximum absorbance) (Table 1). The pK_{cycl} values varied depending on the *N*-alkylation and tended to increase as the *N*-alkyl chain was extended, but all of these HMRs mainly exist in the open form at the physiological pH of 7.4 (>95% for HMDiMeR and HMDiEtR, >80% for HMRG). In contrast, acetylated HMRs exhibited a drastic shift in pK_{cycl} values toward the acidic side (Figures 1b, S2, Table 1): 5.3 for Ac-HMRG, 6.2 for Ac-HMDiMeR, 6.7 for Ac-HMDiEtR, meaning that acetylated derivatives are mainly present in the closed spirocyclic form at physiological pH (>99% for Ac-HMRG, >90% for Ac-HMDiMeR and Ac-HMDiEtR). Interestingly, the values shifted in the same order as the values of the parental HMRs. We speculated that the order of pK_{cycl} values can be explained in terms of the LUMO energy levels of the fluorophores, because they act as electrophiles in the spirocyclization reaction. The LUMO energy levels of the xanthene moieties are summarized in Table 1, and indeed the pK_{cycl} values are linearly correlated with the LUMO energy levels (Figure S3).

Next, we evaluated which of these three derivatives exhibits the best optical properties as a core fluorophore of highly sensitive fluorescence probes for aminopeptidases. We calculated the ratio

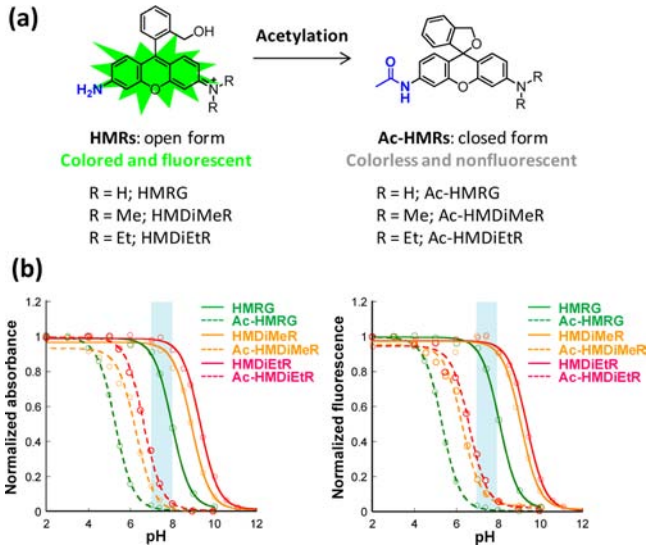

Figure 1. Intramolecular spirocyclization behavior of HMRs and Ac-HMRs. (a) Chemical structures of HMRs (HMRG, HMDiMeR, HMDiEtR) and the corresponding acetylated derivatives, Ac-HMRs (Ac-HMRG, Ac-HMDiMeR, Ac-HMDiEtR). (b) pH dependency of absorbance and fluorescence intensity of HMRs and Ac-HMRs in 0.2 M sodium phosphate buffer at various pH's. Normalized absorbance and fluorescence intensity at wavelengths in parentheses was plotted against pH. HMRG (501 nm, 501/524 nm), HMDiMeR (528 nm, 528/552 nm), HMDiEtR (532 nm, 532/555 nm), Ac-HMRG (495 nm, 495/526 nm), Ac-HMDiMeR (499 nm, 499/571 nm), Ac-HMDiEtR (501 nm, 501/573 nm).

Table 1. Photochemical Properties of HMRs and Ac-HMRs[a]

	absorption maximum (nm)	emission maximum (nm)	fluorescence quantum yield	pK_{cycl}	LUMO level[e] (hartrees)
HMRG	501	524	0.81[a,c]	8.1	−0.2234
Ac-HMRG	495	526	0.27[b,c]	5.3	−0.2336
HMDiMeR	528	552	0.044[a,d]	8.9	−0.2166
Ac-HMDiMeR	499	571	0.02[b,d]	6.2	−0.2266
HMDiEtR	532	555	0.042[a,d]	9.3	−0.2136
Ac-HMDiEtR	501	573	0.01[b,d]	6.7	−0.2235

[a]Measured in 0.2 M sodium phosphate buffer, pH 7.4. [b]Measured in 0.2 M sodium phosphate buffer, pH 2.0. [c]Relative fluorescence quantum yield determined by using fluorescein (Φ_{fl} = 0.85) as a reference. [d]Absolute fluorescence quantum efficiency. [e]LUMO energy level of the corresponding xanthene moiety. Data were calculated at the B3LYP/6-31G level with Gaussian 98W.

dx.doi.org/10.1021/ja309688m | J. Am. Chem. Soc. 2013, 135, 409−414

of the open forms between HMRs and Ac-HMRs and found that HMRG and Ac-HMRG (52-fold) show a much greater difference than other derivatives (13-fold for HMDiMeR and Ac-HMDiMeR, 7-fold for HMDiEtMeR and Ac-HMDiEtR). Further, while HMDiMeR and HMDiEtR showed relatively low fluorescence quantum yields (Φ_{fl}) and short fluorescence lifetimes (τ) in aqueous solution (Φ_{fl} = 0.044, τ = 0.3 ns for HMDiMeR; Φ_{fl} = 0.042, τ = 0.2 ns for HMDiEtR), HMRG had a high fluorescence quantum yield (Φ_{fl} = 0.81) and a long fluorescence lifetime (τ = 3.8 ns) (Table S1). Therefore, the pair of HMRG and acetyl-HMRG seemed to be excellent candidates for producing a strong dynamic fluorescence change in response to enzymatic reaction at the physiological pH of 7.4. This result also demonstrates that it is possible to regulate the fluorescence of rhodamine by controlling intramolecular spirocyclization at a single reactive site. Such precise control cannot be achieved with commercially available RhodamineGreen (RG), as RG and its acetylated derivative (Ac-RG) both show pH-independent high absorbance and fluorescence (Figure S4). On the basis of the above these findings, we next focused on the development of a fluorescence probe for aminopeptidase based on the HMRG scaffold.

To confirm the validity of our new strategy based on HMRG, we chose LAP as a target, because it is well-known to be a clinically significant enzyme that is upregulated in serum of liver disease patients,[13] and it plays important roles in tumor-cell invasion, metastasis, and immune response.[14−16] Thus, rapid and sensitive detection of LAP activity in living samples would have a significant impact in the fields of biology and medicine. According to our strategy, we designed Leu-HMRG by incorporating L-leucine into HMRG via an amide bond (Figure 2a, Scheme S3). The pK_{cycl} value of Leu-HMRG was calculated to be 4.8 (Table 2, Figure S5), meaning that it should exist in the colorless and nonfluorescent closed form at physiological pH, as expected. Next, we tested the reactivity of Leu-HMRG with LAP. The fluorescence intensity and absorbance of Leu-HMRG solution increased drastically following the addition of LAP (Figure 2b), and the fluorescence activation ratio reached more than 400-fold. The fluorescence increase of Leu-HMRG is dose-dependent and linearly related to the amount of LAP (Figure S6). The conversion of Leu-HMRG to HMRG by the enzyme was confirmed by analytical HPLC (Figure S7). Further, other proteases, such as trypsin, chymotrypsin, and cathepsin B, did not increase the fluorescence of Leu-HMRG, demonstrating high specificity of the probe for LAP activity (Figure S8). Moreover, we determined the kinetic parameters of Leu-HMRG and compared the values with those of other commercial LAP substrates, Leu-MCA (L-leucine 4-methylcoumaryl-7-amide, a fluorescent substrate based on AMC[17]) and Leu-pNA (leucyl-*p*-nitroanilide, colorimetric substrate[18]). The k_{cat}/K_m value of Leu-HMRG was 4-fold greater than those of other substrates (Table 3), indicating that Leu-HMRG is a better substrate for LAP than the commercially available substrates. These results indicate that Leu-HMRG is suitable for the sensitive and quantitative detection of LAP activity.

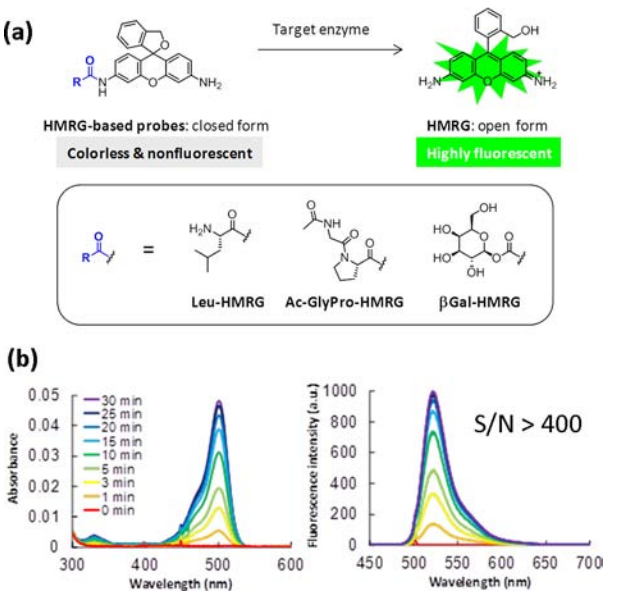

Figure 2. Novel design strategy based on HMRG. (a) Enzymatic reaction of HMRG-based probes with the target enzymes. Leu-HMRG for leucine aminopeptidase (LAP), Ac-GlyPo-HMRG for fibroblast activation protein (FAP), βGal-HMRG for β-galactosidase. (b) Absorption and emission spectra of 1 μM Leu-HMRG at 0, 1, 3, 5, 10, 15, 20, 25, and 30 min after addition of LAP (0.04 U). Reaction was performed in 0.1 M sodium phosphate buffer (pH 7.4) at 37 °C. Excitation wavelength was 501 nm.

Next, we examined the feasibility of applying our probe for diagnostic purposes. As mentioned above, LAP activity in serum is a clinical marker for diagnosis of liver disease. So, we conducted enzyme activity measurement in buffer containing 4% human serum albumin (HSA), the most abundant plasma protein in human blood, to mimic serum. In this experiment, we compared the sensitivity of Leu-HMRG and Leu-MCA. The activation ratio of Leu-HMRG upon addition of 17.5 mU LAP reached 60-fold at 90 min, whereas Leu-MCA showed only 2-fold activation (Figure S9). The reason for the low activation ratio observed with Leu-MCA is considered to be the strong background fluorescence of proteins (HSA) resulting from the UV excitation (Figure S10), and this represents a critical drawback for diagnostic application. In fact, it was quite difficult to detect intrinsic LAP activity in fetal bovine serum with Leu-MCA within a short incubation time, whereas we could sensitively detect the activity with Leu-HMRG (Figure 3). These results clearly indicate the superiority of Leu-HMRG for sensitive detection of LAP activity in the presence of a large amount of proteins, such as in serum, and indicate that Leu-HMRG would be a useful tool for diagnostic purposes.

We next applied Leu-HMRG to detect intracellular LAP activity in living cells. Cytosolic LAP has recently been reported to play an important role in the degradation of peptides for MHC class I binding during an immune response,[19] and its expression is significantly increased in ovarian cancer tissue.[20] When we incubated HeLa cells with Leu-HMRG, we observed a strong fluorescence signal, especially in lysosomes (Figure 4a, Figure S11). To confirm that the obtained signal derives from intracellular LAP activity and to exclude the possibility that unreacted substrate merely accumulated in lysosomes, we performed spectral scanning imaging and inhibitor assay. Spectral scanning showed that the excitation and emission spectra observed in lysosomes coincided with those of HMRG, but not with those of Leu-HMRG, indicating that Leu-HMRG is efficiently converted to HMRG in live HeLa cells (Figure S12). We also performed inhibitor assay by pretreating cells with 2 μM LAP inhibitor, bestatin methyl ester.[21] As a result, the fluorescence increase of Leu-HMRG was clearly blocked (Figures 4b, S13). These results indicate that we can detect intracellular LAP

dx.doi.org/10.1021/ja309688m | J. Am. Chem. Soc. 2013, 135, 409−414

Table 2. Photochemical Properties of HMRG-Based Probes

	absorption maximum (nm)	emission maximum (nm)	fluorescence quantum yield	molar extinction coefficient (M^{-1} cm^{-1})[a]	pK_{cycl}
HMRG	501	524	0.81[a]	57 000	8.1
Leu-HMRG	496	525	0.22[b]	270	4.8
Ac-GlyPro-HMRG	496	527	0.23[b]	340	5.1
βGal-HMRG	494	525	0.32[b]	620	5.4
HMDER[c]	525	543	0.14	80 000	11.3
HMDER- βGal[c]	493, 525	536	0.009	12 000	6.9

[a]Measured in 0.2 M sodium phosphate buffer, pH 7.4. [b]Measured in 0.2 M sodium phosphate buffer, pH 2.0. [c]Reference 8.

Table 3. Comparison of Kinetic Parameters of LAP Probes

	Leu-pNA[a]	Leu-MCA	Leu-HMRG
K_m (μM)	130	103	46
V_{max} (nM/s)	8.6	6.9	13
k_{cat} (s^{-1})	24	19	34
k_{cat}/K_m (s^{-1} μM^{-1})	0.18	0.18	0.75

[a]Leu-pNA (leucyl-*p*-nitroanilide) is a colorimetric substrate for LAP.

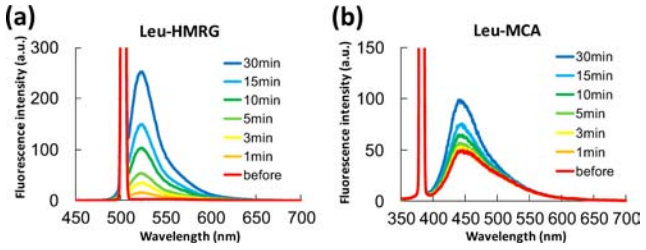

Figure 3. Monitoring LAP activity in fetal bovine serum with Leu-HMRG or commercially available L-leucine 4-methylcoumaryl-7-amide (Leu-MCA). Assays were performed in 50% heat-inactivated fetal bovine serum in PBS, containing 1 μM Leu-HMRG (a) or Leu MCA (b). Excitation wavelength was 501 nm for Leu-HMRG and 380 nm for Leu-MCA.

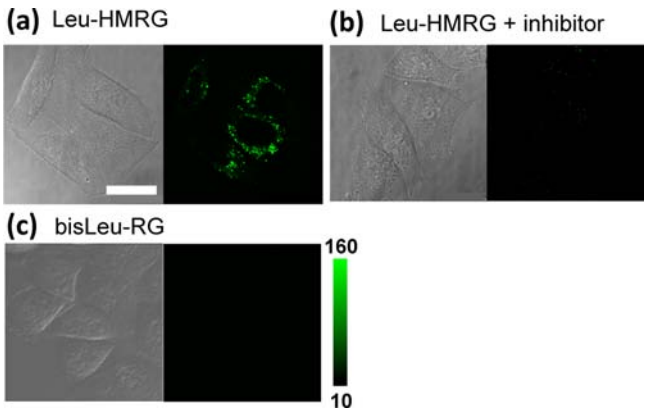

Figure 4. Fluorescence confocal imaging of LAP activity in HeLa cells. (a) Leu-HMRG, (b) Leu-HMRG with inhibitor, (c) bisLeu-RG. Scale bar represents 25 μm.

activity in live cells with Leu-HMRG. Next, we compared the sensitivity of Leu-HMRG with that of bisLeu-RG, a fluorescence probe for LAP activity based on the RG-scaffold, which requires two-step activation (Figure S14a, Scheme S4). In living HeLa cells, bisLeu-RG showed almost no detectable fluorescence, while Leu-HMRG showed strong fluorescence under the same imaging conditions (Figure 4c). Similar results were obtained in cell lysate (Figure S14b). The great difference in sensitivity between the two probes is considered to result from the hydrolysis reaction; bisLeu-RG requires two-step hydrolysis for full fluorescence activation, while Leu-HMRG is fully activated in a single step. Yoon et al. recently reported a LAP-activatable fluorescence probe, DCDHF-Leu, but its fluorescence activation ratio is more than an order of magnitude lower than that of Leu-HMRG (10-fold vs 400-fold), and it requires fixation before imaging in cells.[22] These results show that Leu-HMRG is highly advantageous for fluorescence detection of LAP activity both in living cells and *in vitro*, demonstrating the validity of our approach.

Our design strategy should also be applicable to develop fluorescence probes for other proteases, simply by replacing the leucine moiety of Leu-HMRG with a group specifically susceptible to the protease of interest. Because we have confirmed that HMRG can readily permeate through the cell membrane and accumulate in acidic organelles of living cells, whereas unmodified RG cannot pass through the cell membrane due to its high hydrophilicity (Figure S15), we expected that HMRG would be available as a scaffold for probes targeting membrane-anchored enzymes. On the basis of this idea, we have already employed the strategy described here to develop a fluorescence probe targeting γ-glutamyltranspeptidase (GGT), and used it for cancer imaging based on GGT activity (Figure S16).[23]

To further demonstrate the flexibility of our design strategy, we next focused on different types of targets, that is, dipeptidase and glycosidase. As a dipeptidase, we selected fibroblast activation protein (FAP), which is a cell-surface serine protease that is highly expressed in various carcinomas, such as breast cancer and melanoma.[24] To develop a probe for FAP, a substrate peptide (Ac-GlyPro) was conjugated to HMRG to afford Ac-GlyPro-HMRG (Figure 2a, Scheme S5). As a glycosidase, we selected β-galactosidase, which is widely used as a reporter enzyme to examine transcription or to evaluate transfection efficiency.[25,26] To develop a probe for β-galactosidase, a β-galactoside group was coupled to HMRG via a carbamate linker, affording βGal-HMRG (Figure 2a, Scheme S6). Both Ac-GlyPro-HMRG and βGal-HMRG exhibited almost no fluorescence at physiological pH, due to their spirocyclized structure (Table 2, Figures S17, S18). Upon reaction with FAP or β-galactosidase, respectively, the absorbance and fluorescence intensity of the probes increased quickly and dramatically, and conversion of the probes to HMRG was confirmed by analytical HPLC (Figures S19, S20). We also compared βGal-HMRG with HMDER-βGal,[8] a previously reported fluorescence probe for β-galactosidase based on a rhodol scaffold (Figure S21). The pK_{cycl} value was reduced by more than 1 unit (5.4 for βGal-HMRG, and 6.9 for HMDER-βGal), indicating improved suppression of the background signal (Table 2). Consequently, the fluorescence enhancement upon reaction with the enzyme was larger than that of HMDER-βGal (440-fold for βGal-HMRG vs 76-fold for HMDER-βGal). We also observed a marked fluorescence increase in HEK 293/lacZ cells, while there was no obvious enhancement in HEK 293 cells, which do

dx.doi.org/10.1021/ja309688m | J. Am. Chem. Soc. 2013, 135, 409−414

not express β-galactosidase (Figure 5). Thus, βGal-HMRG could visualize intracellular β-galactosidase activity in living cells and has very favorable features for bioimaging. These results indicate that our design strategy based on precise control of spirocyclization of HMRG is extremely flexible and has the potential to afford highly sensitive probes for a wide range of target enzymes.

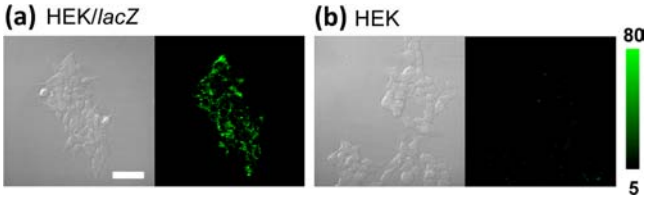

Figure 5. Fluorescence confocal imaging of HEK 293/lacZ cells (a) or HEK 293 cells (b) loaded with βGal-HMRG. Scale bar represents 50 μm.

CONCLUSION

We synthesized a series of rhodamine derivatives bearing a hydroxymethyl group and evaluated their intramolecular spirocyclization behavior. We found that Ac-HMRG exists as a closed spirocyclic structure in aqueous solution at physiological pH, whereas HMRG itself takes an open nonspirocyclic structure. Thus, we concluded that HMRG could be a suitable scaffold to produce a large dynamic fluorescence change via a one-step enzymatic reaction at physiological pH. On the basis of this result, we developed one-step-activatable fluorescence probes for sensitive, selective, and quantitative detection of two aminopeptidases (Leu-HMRG for LAP and Ac-GlyPro-HMRG for FAP), and a glycosidase (βGal-HMRG for β-galactosidase). These probes each exist in the spirocyclic, nonfluorescent form, but are converted to HMRG by the target enzyme, resulting in strong fluorescence activation of up to 400-fold. These probes retain the excellent optical properties of rhodamines, such as brightness and photostability, and offer great practical advantages, including high sensitivity and rapid response; they are expected to be useful for biological and pathological investigations. We anticipate that our design strategy will be applicable to develop probes for a wide range of enzyme activities.

EXPERIMENTAL PROCEDURES

Materials. General chemicals were of the best grade available, supplied by Tokyo Chemical Industries, Wako Pure Chemical, Aldrich Chemical Co., and Invitrogen. They were used without further purification. All solvents were used after appropriate distillation or purification.

Instruments. NMR spectra were recorded on a JEOL JNM-LA300 at 300 MHz for ^{1}H NMR and at 75 MHz for ^{13}C NMR, a JEOL JNM-LA400, or a Bruker AVANCEIII400 Nanobay at 400 MHz for ^{1}H NMR and at 101 MHz for ^{13}C NMR. Mass spectra (MS) were measured with a JEOL JMS-T100LC AccuToF for ESI, or with a MicrOTOF (Bruker). UV−visible spectra were obtained on a Shimadzu UV-1650 and UV-2450. Fluorescence spectroscopic studies were performed on a Hitachi F-4500 and F-7000. Lysate assay on 96-well plates was performed using a plate reader coupled with a Perkin-Elmer LS-55.

Fluorometric Analysis. The slit width of excitation and emission was 5 nm for Ac- HMDiMeR and Ac-HMDiEtR, and 2.5 nm for other compounds and kinetic measurements. The photomultiplier voltage was 700 V. Relative fluorescence quantum efficiency was obtained by comparing the area under the emission spectrum of the test sample excited at 490 nm with that of a solution of fluorescein in 0.1 N NaOH, which has a quantum efficiency of 0.85. Absolute fluorescence quantum efficiency was determined with an absolute PL quantum yield spectrometer, Quantaurus-QY (Hamamatsu Photonics). Fluorescence lifetime was determined with a fluorescence lifetime spectrometer, Quantaurus-Tau (Hamamatsu Photonics).

HPLC Analysis. HPLC analysis was performed on an Inertsil ODS-3 (4.6 × 250 mm) column (GL Sciences Inc.) using an HPLC system composed of a pump (PU-2080, JASCO) and a detector (MD-2010 JASCO). During synthetic procedures, HPLC elution was done with a linear gradient (eluent, 0 min, 20% MeCN/0.1% TFA aq to 15 min, 100% MeCN/0.1% TFA aq; flow rate = 1.0 mL/min). Detection wavelength was 500 nm.

Preparative HPLC. Preparative HPLC were performed on an Inertsil ODS-3 (10.0 × 250 mm) column (GL Sciences Inc.) using an HPLC system composed of a pump (PU-2080, JASCO) and a detector (MD-2010, JASCO).

Kinetic Assay. Various concentrations of the probes (Leu-HMRG, L-MCA, and L-pNA) were dissolved in 0.5 mL total volume of 0.1 M sodium phosphate buffer, pH 7.4, containing 1% DMSO as a cosolvent. LAP (0.7 mU) was added to the solution, and the fluorescence intensity (or absorbance) was recorded continuously as described above. Initial reaction velocity was calculated, plotted against probe concentration, and fitted to a Michaelis Menten curve. The kinetic parameters were calculated by use of the Michaelis−Menten equation shown below:

$$V = V_{max} *[S]/(K_m + [S])$$

where V is initial velocity, and $[S]$ is substrate concentration.

Fluorescence Confocal Microscopy. Fluorescence images were captured using a Leica Application Suite Advanced Fluorescence (LAS-AF) instrument with a TCS SP5 and a 60× objective lens. The light source was a white-light laser. The excitation wavelength was 501 nm (Leu-HMRG) or 577 nm (LysoTracker Red), and the emission wavelength was 510−540 nm (Leu-HMRG and βGal-HMRG) or 585−650 nm (LysoTracker Red). PMT gain: 785 V, offset −0.2%.

Experiments Using Living Cells. HeLa cells, HEK 293 cells expressing β-galactosidase (HEK/lacZ) cells, or those not expressing β-galactosidase (HEK) were cultured in Dulbecco's modified Eagle's medium (DMEM) (Invitrogen Corp.) supplemented with 10% (v/v) fetal bovine serum (Invitrogen Corp.), 1% penicillin, and 1% streptomycin (Invitrogen Corp.) in a humidified incubator containing 5% CO_2 in air.

Evaluation of Fluorescence in Living Cells. Living cells were washed with DMEM supplemented with 1% penicillin and streptomycin three times and incubated at 37 °C with Leu-HMRG (100 nM) or βGal-HMRG (1 μM) for 30 min. After incubation, differential interference contrast and fluorescence images were captured.

Evaluation of Dye Localization in HeLa Cells. HeLa cells were incubated at 37 °C with 100 nM Leu-HMRG and 10 nM LysoTracker Red fluorescent lysosome stain for 30 min. After incubation, differential interference contrast and fluorescence images were captured by confocal microscopy.

Lysate Preparation. HeLa cells were washed twice with 2 mL of DPBS, after reaching 90% confluence. One milliliter of CelLytic (SIGMA) was added, and cells were incubated for 15 min at room temperature on a shaker (180 rpm). The lysed cells were collected with a scraper and centrifuged for 15 min at 16 000g to pellet the cellular debris. The protein-containing supernatant was aliquoted into chilled test tubes and stored at −80 °C.

Lysate Assay on 96-Well Plates. Experiments were performed on black plates (NUNC) at 37 °C. Leu-HMRG or bisLeu-HMRG was added to 0.1 M sodium phosphate buffer (pH 7.4). Next, 0.02 mL of cell lysate was added to the well (total volume 0.2 mL). The plates were incubated for 30 min. The fluorescence intensity (ex 478−492 nm, em 523−548 nm) was measured.

ASSOCIATED CONTENT

Supporting Information

Synthesis and characterization of compounds, pH profiles, fluorescence imaging, lysate assay, and experimental details.

dx.doi.org/10.1021/ja309688m | J. Am. Chem. Soc. 2013, 135, 409−414

This material is available free of charge via the Internet at http://pubs.acs.org.

AUTHOR INFORMATION

Corresponding Author

tlong@mol.f.u-tokyo.ac.jp; uranokun@m.u-tokyo.ac.jp

Notes

The authors declare no competing financial interest.

ACKNOWLEDGMENTS

This research was supported in part by a Grant-in-Aid for Scientific Research (Specially Promoted Research 22000006 to T.N.), by the Ministry of Education, Culture, Sports, Science and Technology of Japan (Grants for The Advanced and Innovational Research Program in Life Sciences, 16370071 and 16659003, Grants 20117003 and 23249004 to Y.U., and 23113504 to M.K.), by The Mochida Memorial Foundation for Medical and Pharmaceutical Research (grants to M.K.), and by The Tokyo Society of Medical Sciences (grants to M.K.).

REFERENCES

(1) Artal-Sanz, M.; Tavernarakis, N. *FEBS Lett.* **2005**, *579*, 3287−3296.
(2) Schäfer, C.; Fels, C.; Brucke, M.; Holzhausen, H. J.; Bahn, H.; Wellman, M.; Visvikis, A.; Fischer, P.; Rainov, N. G. *Acta Oncol.* **2001**, *40*, 529−535.
(3) Ishii, K.; Usui, S.; Sugimura, Y.; Yoshida, S.; Hioki, T.; Tatematsu, M. *Int. J. Cancer* **2001**, *92*, 49−54.
(4) Azaryan, A. V.; Hook, V. Y. *FEBS Lett.* **1994**, *341*, 197−202.
(5) Drag, M.; Bogyo, M.; Ellman, J. A.; Salvesen, G. S. *J. Biol. Chem.* **2010**, *285*, 3310−3318.
(6) Hug, H.; Los, M.; Hirt, W.; Debatin, K. M. *Biochemistry* **1999**, *38*, 13906−13911.
(7) Kenmoku, S.; Urano, Y.; Kojima, H.; Nagano, T. *J. Am. Chem. Soc.* **2007**, *129*, 7313−7318.
(8) Kamiya, M.; Asanuma, D.; Kuranaga, E.; Takeishi, A.; Sakabe, M.; Miura, M.; Nagano, T.; Urano, Y. *J. Am. Chem. Soc.* **2011**, *133*, 12960−12963.
(9) Liu, W.; Xu, L.; Zhang, H.; You, J.; Zhang, X.; Sheng, R.; Li, H.; Wu, S.; Wang, P. *Org. Biomol. Chem.* **2009**, *7*, 660−664.
(10) Zheng, H.; Shang, G. Q.; Yang, S. Y.; Gao, X.; Xu, J. G. *Org. Lett.* **2008**, *10*, 2357−2360.
(11) Zheng, W.; Tang, B.; Liu, X.; Liu, Y.; Xu, K.; Ma, J.; Tong, L.; Yang, G. *Analyst* **2009**, *134*, 367−371.
(12) Pires, M. M.; Chmielewski, J. *Org. Lett.* **2008**, *10*, 837−840.
(13) Mericas, G.; Anagnostou, E.; Hadziyannis, S. T.; Kakari, S. *J. Clin. Pathol.* **1964**, *17*, 52−55.
(14) Pilar, C. M.; Ramírez-Expósito, M. J.; Dueñas, B.; Dolores, M. M.; Jesús, G. M.; De la Chica, S.; Cortés, P.; Ruíz-Sanjuan, M.; Martínez-Martos, J. M. *Anticancer Res.* **2006**, *26*, 1011−1014.
(15) Mizutani, S.; Shibata, K.; Kikkawa, F.; Hattori, A.; Tsujimoto, M.; Ishii, M.; Kobayashi, H. *Expert Opin. Ther. Targets* **2007**, *11*, 453−461.
(16) Saric, T.; Chang, S. C.; Hattori, A.; York, I. A.; Markant, S.; Rock, K. L.; Tsujimoto, M.; Goldberg, A. L. *Nat. Immunol.* **2002**, *3*, 1169−1176.
(17) Kanaoka, Y.; Takahashi, T.; Nakayama, H. *Chem. Pharm. Bull.* **1977**, *25*, 362−363.
(18) Lapp, C. A.; O'Conner, J. L. *Biol. Reprod.* **1984**, *30*, 848−54.
(19) Beninga, J.; Rock, K. L.; Goldberg, A. L. *J. Biol. Chem.* **1998**, *273*, 18734−18742.
(20) Shibata, K.; Kajiyama, H.; Mizokami, Y.; Ino, K.; Nomura, S.; Mizutani, S.; Terauchi, M.; Kikkawa, F. *Gynecol. Oncol.* **2005**, *98*, 11−18.
(21) Sekine, K.; Fujii, H.; Abe, F.; Nishikawa, K. *Int. J. Cancer* **2001**, *94*, 485−491.
(22) Yoon, H. Y.; Shim, S. H.; Baek, L. J.; Hong, J. I. *Bioorg. Med. Chem. Lett.* **2011**, *21*, 2403−2405.
(23) Urano, Y.; Sakabe, M.; Kosaka, N.; Ogawa, M.; Mitsunaga, M.; Asanuma, D.; Kamiya, M.; Young, M. R.; Nagano, T.; Choyke, P. L.; Kobayashi, H. *Sci. Transl. Med.* **2011**, *3*, 110−119.
(24) Huang, Y.; Wang, S.; Kelly, T. *Cancer Res.* **2004**, *64*, 2712−6.
(25) Alam, J.; Cook, J. L. *Anal. Biochem.* **1990**, *188*, 245−254.
(26) Spergel, D. J.; Kruth, U.; Shimshek, D. R.; Sprengel, R.; Seeburg, P. H. *Prog. Neurobiol.* **2001**, *63*, 673−686.